Arabian Journal for Science and Engineering (2022) 47:6341–6353
https://doi.org/10.1007/s13369-021-06020-9

RESEARCH ARTICLE-CHEMICAL ENGINEERING

Magnetic Nano-catalyzed Synthesis of Biodiesel from Tannery Sludge: Characterization, Optimization and Kinetic Studies

Vijaya Kumar Booramurthy[1] · Ramesh Kasimani[2] · Sivakumar Pandian[3] · Deepalakshmi Subramanian[4]

Received: 3 February 2021 / Accepted: 28 July 2021 / Published online: 6 November 2021

Abstract

The fat extracted from tannery sludge was utilized for producing biodiesel by transesterification reaction using a short chain alcohol and a nano-catalyst (Fe_3O_4/BaO). This catalyst was synthesized through co-precipitation method and various characterization techniques were followed using analytical instruments. The synthesized catalyst was examined through transesterification reaction using tannery sludge fat for observing the activity performance. The effect of various process parameters was investigated to obtain an optimum yield of 97.6%. The optimum reaction conditions were 18:1 molar ratio of methanol/oil, 8 wt% of catalyst loading with 65 °C of reaction temperature, 300 min of reaction time and a rate of stirring of 450 rpm. Furthermore, the ASTM standard test methods were followed for examining the fuel property of biodiesel and were found to be within the range of ASTM D6751 standard. Moreover, the rate of reaction (k') was determined by conducting the kinetic studies. The obtained values of 46.64 kJ mol^{-1} and 21.3×10^3 min^{-1}, respectively, denote activation energy and frequency factor.

Keywords Biodiesel · Nano-catalyst · Co-precipitation · Transesterification · Kinetics

1 Introduction

The non-renewable sources such as petroleum, natural gas and coal are unavoidably needed for the growth of the nation around the globe. Recently, it has been reported that the increase in usage of fossil fuels raised the concern about the environmental pollution, which in turn leads to greenhouse gas emissions[1, 2]. These issues can be overcome by developing alternative fuels, which are of renewable, sustainable and effectively enhance the energy availability. In the past, renewable fuel such as vegetable oil was directly used in a diesel engine as an alternative for petroleum diesel. From the development of engine era, the source of energy utilized by diesel engines was vegetable oil. In 1900, Rudolph diesel used peanut oil as a source of energy to drive the first diesel engine in the Paris World Exhibition. The restriction to use vegetable oil as a source for diesel engine was initiated due to its higher viscosity which leads to low performance of the engine. In order to replace the existing source of energy, biofuel, which has been providing greater potential comparable to petroleum sources will be a best option for alternate fuel. In that way, biodiesel has generated positive impact toward the environment by its advantageous effect such as non-toxic, biodegradable, lesser emission and environment friendliness [3]. The liquid fuel is derived from various feedstocks, such as vegetable oil (both edible and non-edible), animal fat, waste cooking oil industrial grease and micro-algae. Different methods such as pyrolysis, dilution, micro-emulsion and transesterification were followed for lowering the viscosity of the feedstock for producing biodiesel. Transesterification method was adopted as a best technique when compared to the other methods for decreasing the viscosity of oil as well as to operate at moderate temperature. The reaction between triglycerides of vegetable oil or animal fat and alcohol with the help of a catalyst to produce biodiesel and glycerol as a by-product is known as transesterification. Commonly, three different catalysts

✉ Vijaya Kumar Booramurthy
dbsvijayakumar@gmail.com

1 Department of Petrochemical Engineering, RVS College of Engineering and Technology, Coimbatore 641402, India

2 Department of Mechanical Engineering, Government College of Technology, Coimbatore 641013, India

3 School of Petroleum Technology, Pandit Deendayal Energy University, Gandhinagar 382426, India

4 Department of Engineering and Physical Sciences, Institute of Advanced Research, Gandhinagar 382426, India

such as base catalyst, acid catalyst and enzyme catalyst were utilized for this reaction.

The total production cost of biodiesel is comparatively higher than petro-diesel, which leads to major disadvantage based on economic concern. It was noted that 75 to 80% of the total cost is entirely based on the raw material [4]. So, the selection of feedstock for producing biodiesel is one of the important aspects. The most possible way is to choose a low-cost as well as effective feedstock, which includes animal fat, waste cooking oil, industrial grease, fish oil, tannery sludge and non-edible [5].

In leather industries, huge amount of tanning waste is produced from the raw hide during the pretreatment. These tanning wastes lead to environmental pollution concerning water emission, terrestrial and ecosystem damage [6]. The feedstock produced from tannery sludge was recommended as a low cost, which in turn produces biodiesel in a cost-effective manner. But this feedstock contains excess amount of lipids and proteins, which is very difficult to separate. The presence of protein in the feedstocks holds enormous number of amino acids bonded together with polypeptide. The hydrolysis processes were carried out in order to make the interaction of amino acids to separate the fat and protein by the application of heat [7, 8]. It has been observed by the author that the vegetable oil and waste fat considerably contain excess amounts of protein apart from fat; the challenge required here is to remove the presence of protein from the fat through refining process (physical and chemical treatment) [9]. These waste fats possess an adequate amount of free fatty acid, which can be extracted for the production of biodiesel. The most significant possible way of using this contaminated feedstock with cost-effective homogeneous catalyst in industrial scale will lead to soap formation and difficulty in product separation. The presence of fatty acid in feedstock for utilization of homogeneous catalyst should have acid value less than 1 mg KOH g^{-1}, but the feedstocks (tannery sludge) contain free fatty acid content above it. Therefore, many researchers have been focusing in the way of producing a heterogeneous catalyst, which is not influenced by the presence of impurities as well as utilization of lesser amount of water during the separation process [9].

The use of heterogeneous catalyst for the production of biodiesel results in lowering the time during the separation of catalyst from the product and provides better results in reusability studies [10, 11]. But, the major concern in the utilization of heterogeneous catalyst results in slow reaction rate due to the three-phase existences which lower the mass transfer between the reactants.

Recently, magnetic heterogeneous nano-catalysts have been providing better catalytic activity through its higher surface area promoting toward adequate mass transfer. This evidence regarding magnetic nano-catalyst in the catalysis field initiates to develop a larger surface area, recovery of catalyst through permanent magnet and reused for several cycles [10, 12]. However, most of the research is carried out for recovering the heterogeneous catalyst through mechanical operations such as filtration or via centrifuging, where by magnetic nano-catalyst has promoted an easy separation process with a help of magnetic field. Eventually, magnetite is promptly used for producing magnetic nanoparticles due to its higher tensile strength, reactivity and non-toxicity [13]. These magnetic nanoparticles have been used in various industrial applications in the preparation of fine chemicals and pharmaceutical products, drug synthesis, food additives, biochemical and in other sectors [14, 15]. It has been utilized in different biomedical applications for the development of MRI (magnetic resonance imaging), health care and in the field of biotechnology, etc. [16]. Feyzi et al. reported a novel magnetic catalyst $Ca/Fe_3O_4@SiO_2$ showed higher catalytic activity for producing biodiesel from sunflower oil yielding 97%. The biodiesel conversion of 99.9% achieved using a nano-catalyst $Mg/ZnFe_2O_3$ from waste cooking oil was reported showing that the catalyst exhibits higher recovery during the separation [17]. The catalyst performed well in the transesterification reaction, holding higher magnetic property, provides an effective platform in the separation after the completion of the reaction by utilizing a permanent magnet [18]. The preparation of nano-catalyst with the impregnation of magnetic core effectively reduces the problem in the recycling as well promotes better reusability with less deactivation of the active sites of the catalyst [19]. It has been reported that the magnetic nanoparticles support over graphene oxide exhibits higher surface area, providing effective separation of magnetic properties [20]. The catalytic performance was improved to 85% through the impregnation of calcium oxide with iron during the transesterification reaction providing enhancement in the active sites of the catalyst [21]. Similarly, Vijayakumar et al. utilized magnetic nano-catalyst Fe_3O_4/Cs_2O for generating biodiesel from tannery waste at optimum yield of 97.1%. Liu et al. developed a nano-catalyst CaO/Au provided superior catalytic activity toward transesterification reaction to convert soya bean oil into biodiesel producing a yield of 88.9%.

In the present investigation, magnetic nano-catalyst (Fe_3O_4/BaO) was prepared through wetness impregnation method. The catalytic activity was determined through transesterification reaction of a low-cost feedstock with methanol and nano-magnetic catalyst. The characterization of the synthesized catalyst was carried out by Fourier transform infrared spectroscopy (FTIR), X-ray diffraction (XRD), scanning electron microscopy (SEM), VSM (vibrating sample magnetometer) and particle analyzer, as well as the catalyst stability was also carried out for identifying the number of cycles in which the catalyst has been reused. The optimization was investigated with respect to the various process parameters initiated for biodiesel production. The physical

and chemical properties of the extracted fat were examined as per standard methods and the final product biodiesel was characterized and compared with ASTM D6751 standard.

2 Materials and Methods

The leather tannery sludge produced through skinning and fleshing operation was collected from the tanning industry located in Ranipet, Tamil Nadu, India. The pretreatment is carried in order to remove the presence of considerable amounts of impurities other than FFAs, additionally the existence of protein, water and phosphatides through the refining process. The degumming is the process in which the level of phosphatides will be reduced. Further processing is done through steam refining for the reduction of FFAs and water content from the feedstock by utilizing vacuum distillation [9]. The obtained sludge was dried at 110 °C for reducing the level of moisture content and placed in an airtight container for further process. The crushing operation was done in laboratory for obtaining a uniform mixture, then after extraction process was carried out for 8 h via Soxhlet apparatus. Petroleum hexane was used as a solvent for extraction purposes. The solvent was removed after the extraction process by using vacuum distillation and kept for drying in a hot air over at 105 °C. The gravimetric method was followed for determining the yield of fat from the tannery sludge by using Eq. (1)

$$\text{Fat yield} = \frac{\text{weight of the fat extracted}(g)}{\text{weight of the dried tannery sludge}(g)} \times 100. \quad (1)$$

The AOAC standard method was followed in determining the physical and chemical properties of the tannery waste fat. The chemicals and reagents utilized for the study were of analytical grade bought from Sri Sastha Scientific Company, Coimbatore, Tamil Nadu, India.

The identification of the different fatty acids was carried out using GC (gas chromatography). The GC equipment, Agilent 7820A model, fitted with HP-5 capillary column coupled with ionization detector was utilized for the determination of fatty acid methyl ester content (wt%). A pretreatment of methylation process was carried out for the sample before using it in GC. The chromatographic conditions applied for the inlet and detector temperature were maintained at 260 °C, the inert gas was utilized as a carrier gas flowing at a rate of 1 mL min^{-1}, and split injection ratio was maintained at 50:1. The composition of the fatty acid was identified with respect to the retention time as per the chromatographic standard and eventually match with the peak area of the fatty acid methyl ester. The fatty acid profile is mainly utilized for calculating the average molar mass of the fat by following Eq. (2).

$$\text{Average molar mass of the fat} = 3\sum\left(MW_iX_i\right) + 38 \quad (2)$$

$$\text{Average molar mass of the fat} = 3\sum\left(MW_iX_i\right) - \text{Molecular weight of glycerol} + 3(\text{molecular weight of water})$$

$$\text{Average molar mass of the fat} = 3\sum\left(MW_iX_i\right) - 92 + 3(18).$$

For estimating the molecular weight of sludge, the individual fatty acid molecular weight value was taken to multiply with their mole fraction and then the entire value was multiplied by 3. The average molar mass of the fat value was calculated from the different fatty acid compositions given in Table 2. This value can be used in determining the conversion biodiesel, where MW_i represents the average molar mass and Xi represents mole fraction of the i^{th} fatty acid.

2.1 Preparation of Fe_3O_4

The magnetite (Fe_3O_4) was prepared via co-precipitation method, (a two-step process involving nucleation, which takes place quickly until supersaturation and slowly through diffusion, in which solutes were displaced over the surface of the catalyst) in which 15 g of Fe_2SO_4. $4H_2O$ and 30 g of $FeCl_3$. $6H_2O$ were taken separately in a 250-mL beaker with distilled water. The prepared solution was poured into a 1000-mL beaker and was kept over a hot plate with magnetic stirrer for continuous mixing, maintained at a temperature above 65 °C with a stirring rate of 450 rpm. To this mixture, cetyltrimethyl-ammonium bromide was added in order to develop a colloidal suspension during the reaction. During the reaction, sodium hydroxide of 0.1 N was added in dropwise until a pH value 10 was reached; thereafter, the mixture was stirred without any disturbance for 1 h by maintaining a temperature of 70 °C. A solid black-colored magnetite precipitate was obtained and separated with the aid of a permanent magnet [3, 22].

2.2 Preparation of BaO

Barium chloride was taken in a 250-mL beaker with deionized water and the mixture was stirred continuously to which ammonia solution was added gradually until it reaches a pH value of 10. Then, after the addition of ammonia was stopped and the mixture was stirred by maintaining at 60 °C. The resultant white-colored precipitate was obtained through

filtration and washed with distilled water. The obtained product was dried in an oven for 2 h at 110 °C and calcinated for 3 h at 400 °C in a muffle furnace.

2.3 Impregnation of BaO with Magnetic Nano-core

A known concentration of barium oxide was transferred into a beaker of 500 mL containing a mixture of Fe_3O_4 dispersed with ethanol, deionized water and cetyltrimethylammonium bromide. The mixture was continuously mixed by placing it over a magnetic stirrer with hot plate for 1 h at 65 °C. Thereafter, the dried magnetic nanoparticle was calcinated in a muffle furnace for 2 h at 500 °C. The final product was cooled and the magnetized material was removed by utilizing a permanent magnet. The produced magnetic nano-catalyst was further utilized for producing biodiesel.

2.4 Characterization of Fe_3O_4/BaO

The precursor and morphology of the catalysts were observed using scanning electron microscopy. The Quanta 250 FEG (Thermo Fisher Scientific, USA) instrument was utilized for getting the structured image and FTIR spectrometer was used for identifying the presence of functional group in the catalyst. The Spectrum Two PerkinElmer Spectrometer (USA) was handled for retrieving spectrum, which is observed by using a universal attenuated total reflection sampling techniques and was reported in between the scanning range of 400 and 4000 cm^{-1}.

The instrument (X'pert Pro model PAN analytical diffractometer instrument) was employed for identifying and recording the XRD pattern of the catalyst by using a Cu Kα radiation source in the 2θ range from 20° to 80° with a step size of 0.02°. The Debye–Scherrer's relationship was employed for determining the average crystallite size of the particle as shown in Eq. (3).

$$D = \frac{0.9\lambda}{\beta cos\theta} \tag{3}$$

where θ is the diffraction angle, β is the full width at half maximum, λ is the X-ray wavelength and D is the average crystallite size.

The instrument used for determining the particle size distribution of the prepared catalyst was carried out by Mastersizer 3000 laser scattering particle size analyzer (Malvern Instrument Ltd., Worcestershire, UK). Before the analysis, short chain alcohol was chosen for dispersing the particles and sonicated for 5 min to form a stable wet suspension. The particle sizes ranging between 10 and 3.5 nm were measured. A VSM (vibrating sample magnetometer) was utilized for determining the magnetic behavior of the prepared catalyst. The analysis was carried out by using a magnetometer to which a sample of magnetic nanoparticle was kept suspended. The samples were measured by the magnetometer in between the magnetic field −0.7 T and + 0.7 T at 27 °C.

2.5 Transesterification Process

Fat extracted from tannery sludge, methanol and catalyst were added into a 250-mL three-neck round-bottom flask for the reaction to take place, in which one neck was connected with condenser in order to condense the evaporated methanol during the reaction, the thermometer was connected to the second neck for recording the temperature with respect to the start of reaction, and the last neck is utilized for adding the reactants into the reactor. The whole reactor setup was kept over a hot plate magnetic stirrer in which the reaction was carried out under a constant stirring rate. Initially, the fat which was in solid form at room temperature was heated at 40 °C to be in liquid phase and was poured into the round-bottom flask for every experiment. The fat was preheated with varying temperature from 40 to 80 °C to which a mixture of catalyst and methanol was added. For carrying out the optimization studies, various process parameters were taken such as methanol/fat molar ratio of (6:1 to 30:1), catalyst loading of (3–10 wt%) and reaction time of (1–6 h) were changed. The optimization was followed by one-factor-at-a-time method, in which only one parameter is about to vary and remaining parameters were constant. The selected variable concentrations were varied over a preferred range.

During the completion of the reaction, stirring was stopped and the resultant mixture was collected and was allowed to cool. A permanent magnet was utilized for removing the catalyst from the resultant mixture. Then, the cooled mixture was poured into a separating funnel for separating the final product. The separation was carried out without any disturbance for 12 h which forms two different layers, product biodiesel was at the top, and the by-product glycerol was at the bottom. The biodiesel was recovered from the top of the separating funnel and bottom layer was transferred into a rotary vacuum evaporator for the removal of methanol [23]. Then, the yield of biodiesel was calculated gravimetrically by following Eq. (4) [24]

$$\text{Biodiesel yield(wt\%)} = \frac{\text{Weight of biodiesel } (g)}{\text{Weight of fat}(g)} \times 100. \tag{4}$$

The conversion of fatty acid methyl ester from fat was analyzed using H^1NMR (Proton Nuclear Magnetic Resonance Spectroscopy) (Bruker AVANCE III 500 MHz). The analysis was carried out by dissolving the sample in $CDCl_3$ and the sample was operated at 298 K. It was observed that the

presence of singlet peak of methoxy protons and triplet peaks of alpha-methylene protons of methyl ester in the spectrum will be examined for determining the conversion of methyl esters by following Eq. (5) [8]

$$\text{Conversion} = \frac{2A_1}{3A_2} \times 100 \tag{5}$$

where A_1 is the integration of methoxy protons and A_2 is the alpha-methylene protons of methyl esters,

Produced product biodiesel was evaluated by using ASTM standard methods and the comparison was made with ASTM D6751 standards. For each and every experiment, triplicate evaluation was carried out by utilizing the result obtained from reproducibility and further standard deviation was investigated.

3 Results and Discussion

3.1 Catalyst Characterization

3.1.1 SEM Analysis

The displayed Fig. 1a and b confirms the SEM image of Fe_3O_4 and Fe_3O_4/BaO, respectively. It was indicated that the observation identifies morphology of the calcined catalyst with and without magnetite. The magnetic particles which are formed seem to be agglomerated possessing larger surface area due to lesser attraction between the particles. It shows that the particles are being smaller and possess regular arrangement, which revealed that the magnetic particle has lesser agglomeration. On impregnating barium oxide over the magnetite particle, increasing in surface area was well observed and seems to form a different structure, where the barium oxide particle was strongly dispersed over the surface of magnetite.

3.1.2 FTIR Analysis

The presence of functional groups of the synthesized nano-catalyst was quantitatively analyzed by identifying the presence of peaks through FTIR analyzer (Fig. 2). It was identified that the characteristic of metal oxide seems to be adsorbed strongly showing the vibration band tending to be tetrahedral and octahedral stretching at a range of 550 and 650 cm^{-1}, respectively [25]. The presence of BaO was observed in the peak at 1620 cm^{-1} which is attributed toward the stronger position of magnetite. The adsorption of water molecule over the surface of the nano-catalyst was observed in the peak range of 3390 cm^{-1} which is due to O–H stretching in the nano-catalyst [3, 26].

3.1.3 XRD Analysis

The X-ray diffraction pattern was observed for Fe_3O_4/BaO, showing that the barium oxide was covered strongly over the surface of the magnetite. The peak value that corresponds to 2θ range for barium oxide was (17.21°, 30.35°, 43.45°, 54.21° and 68.23°) found to possess the centered position of the nano-catalyst. The presence of iron oxide exhibits

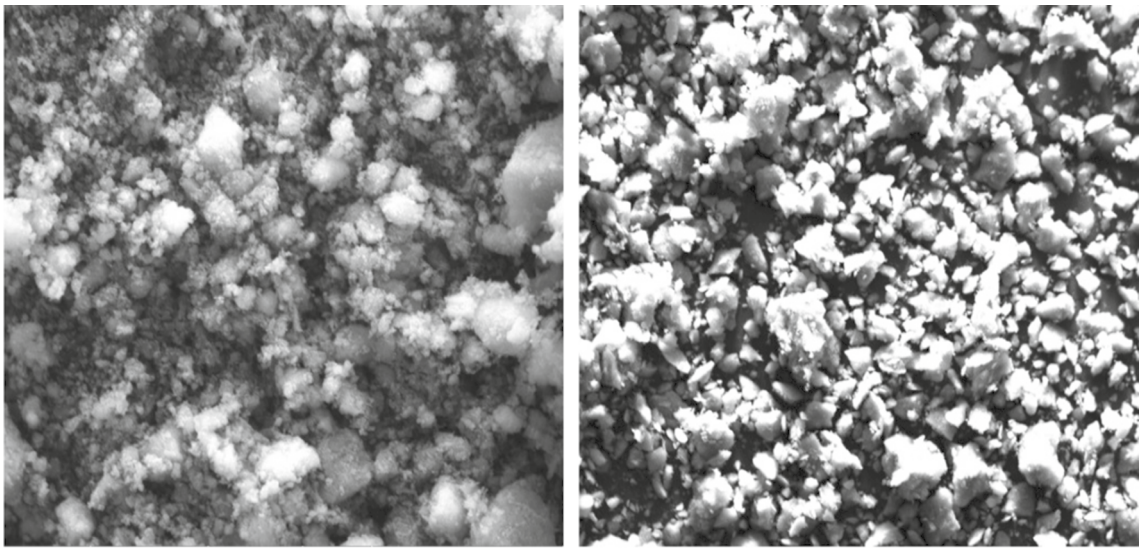

(a) SEM image of Fe_3O_4 (b) SEM image of Fe_3O_4/BaO

Fig. 1 **a** SEM image of Fe_3O_4. **b** SEM image of Fe_3O_4/BaO

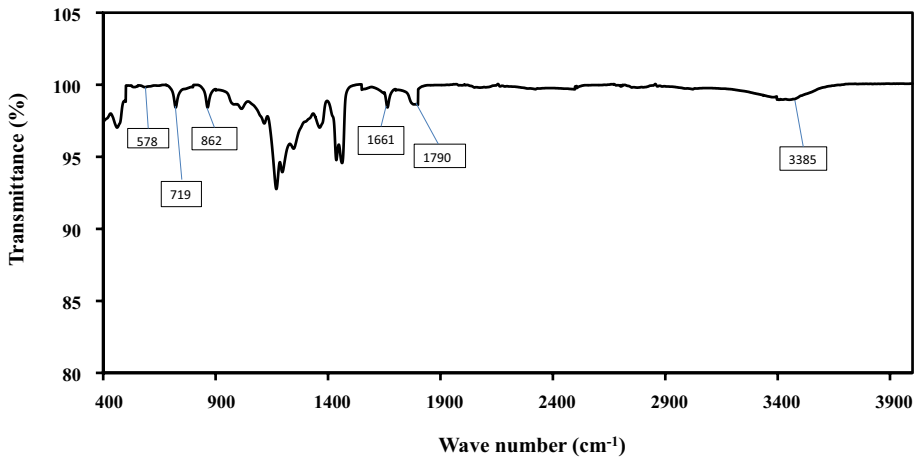

Fig. 2 FTIR spectrum of Fe_3O_4/BaO

inverse spinal structure which is well observed at 38.39º and 60.47° (Fig. 3). The similar result was observed showing strong and sharp peaks for the presence of iron oxide at 2θ (30.2°, 35.6°,43.7°,57.3° and 6.2.9°) [27]. The magnetite core is confined and is not affected by adherence of barium oxide on to the surface. The pattern shows that Fe_3O_4/BaO withstands longer retention holing spinal structure during the barium coating process. The structure is sustained well, showing that the particle size of nano-catalyst is generally in the form of nano-dimension which is obtained through Debye–Scherrer's relation and found to be in the range of 20–80 nm.

The ability of the catalyst to undergo dispersion in micro-level during the reaction enables to distribute the reactant particles and found that the magnetite particles were well distributed in the reaction showing tapered form holding 95% of the particles in the range between 20 and 80 nm and Fe_3O_4/BaO exhibit wide distribution of particle in the range between 20 and 100 nm.

The synthesized catalyst was analyzed for determining the magnetic property through VSM. The identification of the magnetic behavior of the catalyst was examined by hysteresis curve. It was examined that the strength of ferromagnetic property was lower at initial stage, which in turn lowers the saturation magnetization value and upon increasing the temperature the ferromagnetic strength gets stronger inducing higher value of saturation magnetization. The saturation magnetization for Fe_3O_4 and Fe_3O_4/BaO was found to be 35 emu g^{-1} and 15 emu g^{-1}. Comparatively, the magnetite doped with BaO induces higher saturation magnetization value toward magnetite-doped cesium oxide and calcium oxide doped with magnetite coupled silicon dioxide [3, 22]. It was observed that the difference in saturation magnetization was due to thermal treatment toward synthesizing the catalyst as well as with respect to the particle interaction between the core magnetite and barium oxide. The magnetic property of the magnetite core was not affected due to impregnation of BaO, which could possibly enhance the

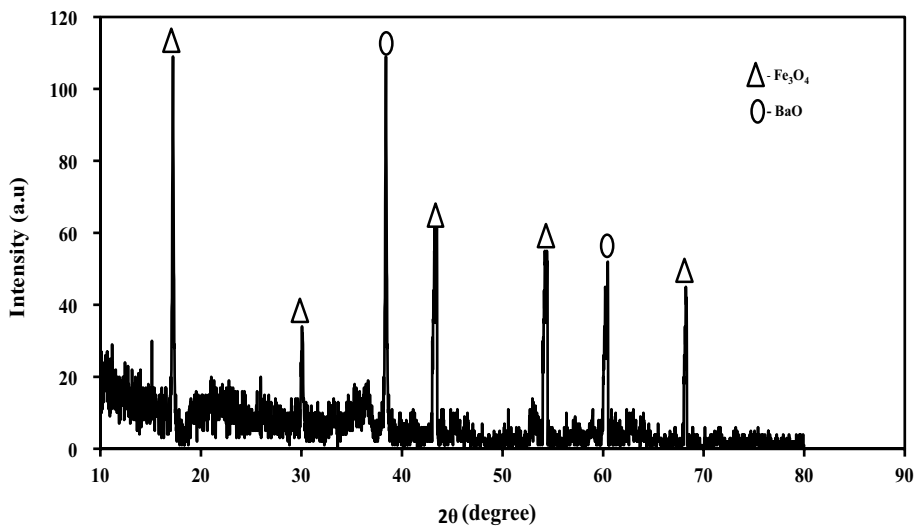

Fig. 3 XRD spectrum of Fe_3O_4/BaO

catalytic property during the transesterification reaction [28]. But the difference is value of saturation magnetization that depends on the magnetic strength of the fresh magnetic nano-catalyst and the reused catalyst was observed. During the washing and leaching process, the active sites of the catalyst may lead to decrease which in turn reduces the magnetic strength. It is also observed that the portion of barium oxide is adsorbed over the magnetite. The magnetic property of the catalyst provides a narrow size distribution of the particles holding strong superparamagnetic behavior. This provides the path way to get the magnetic particles to be strongly agglomerated.

3.2 Characterization of Extracted Fat

A 35.5 wt% dried fat was produced from tannery sludge. The raw fat was solid at room temperature, appearing to be pale yellow. In Table 1, various properties of the fat are listed. The iodine value of the fat was found to be 42 g I_2 100 g^{-1} indicating that this fat falls under the category of drying oil which can be easily solidifies at 27 ºC. It is confirmed that iodine value is typically based on the degree of unsaturation in the fatty acid molecule which founds to be lower than other edible and non-edible oils possessing good oxidative stability [29]. The acid value is found to be lower and indicates that the FFA content is 2.26%, which confirms that the extracted raw material tannery sludge is well suitable for producing biodiesel using Fe_3O_4/BaO [24].

The fatty acid profile for the extracted tannery sludge was examined through GC analysis. In Table 2, the presence of various fatty acids of the fat is listed. The determination of saturated, mono-saturated and poly-saturated was calculated from the fatty acid profile list. It has been clearly identified that the fat contains 59.44% of saturated, 36.42% of mono-saturated and 3.44% poly-saturated fatty acids. From the various compositions of fatty acid, saturated fatty acid possesses higher value, which enhances the cetane numbers and calorific value as well as resists to oxidation and polymerization. The mass ratio of saturated to unsaturated was found to be 1.49, which promotes the biodiesel to solidify at cold climatic conditions due to low-temperature characteristics. From the fatty acid profile, average molecular weight of the fat was calculated and was found to be 859.8 g mol^{-1} showing higher level of saturated fatty acid.

Table 1 Physiochemical properties of fat extracted from tannery sludge

Property	Units	Fat
Iodine number	g I_2 100 g^{-1}	43.54
Density	kg m^{-3}	920
Kinematic Viscosity@40 °C	mm^2 s^{-1}	46
Acid number	mg KOH g^{-1}	4.5
Water content	wt%	0.28
Melting point	°C	47

Table 2 Fatty acid profile of fat extracted from tannery sludge

Fatty acid	Carbon number	Fat
Stearic acid	C18:0	31.21
Oleic acid	C18:1	36.42
Myristic acid	C14:0	4.25
Palmitic acid	C16:0	23.8
Linolenic acid	C18:3	0.24
Linoleic acid	C18:2	3.2
Arachidic acid	C20:0	0.18
Undetectable		0.7

3.3 Optimization of Biodiesel

3.3.1 Effect of Methanol to oil Molar Ratio

It is one of the most influencing parameters, which affects the conversion of biodiesel during the transesterification process. Many researches proved that the reaction is carried out above the stoichiometric limit of utilizing methanol with oil, which will enhance the rate of diffusion between the reactants thereby increasing the yield by shifting the equilibrium reaction toward forward reaction. Here, the optimization of biodiesel yield was examined by varying the methanol-to-oil molar ratio from 5:1 to 20:1 during the reaction. Increasing the methanol-to-oil molar ratio increases the biodiesel production yield. It has been identified that the reaction starts slowly at 5:1 molar ratio providing a yield of 58 wt% and continuously increases to 76 wt% at 18:1 methanol to oil molar ratio (Fig. 4a). Further, increase in the addition of methanol during the reaction leads to solubility factor (excess methanol tends to completely dissolve with glycerol, which restricts the further progression of the reaction, that makes very difficult for separating the product and by-product) [30], which makes difficult during separation of by-product as well as tends to reverse the reaction. Apparently increasing the concentration of methanol, above 18:1 molar ratio during the reaction will tend to reduce the yield of biodiesel slightly [31]. Thus, the optimum methanol-to-oil molar ratio was found to be 18:1 which is comparatively lower than by the use of magnetite-doped cesium oxide [3].

3.3.2 Effect of Catalyst Loading

The most important aspect of biodiesel production is the catalyst loading. This parameter influences the biodiesel

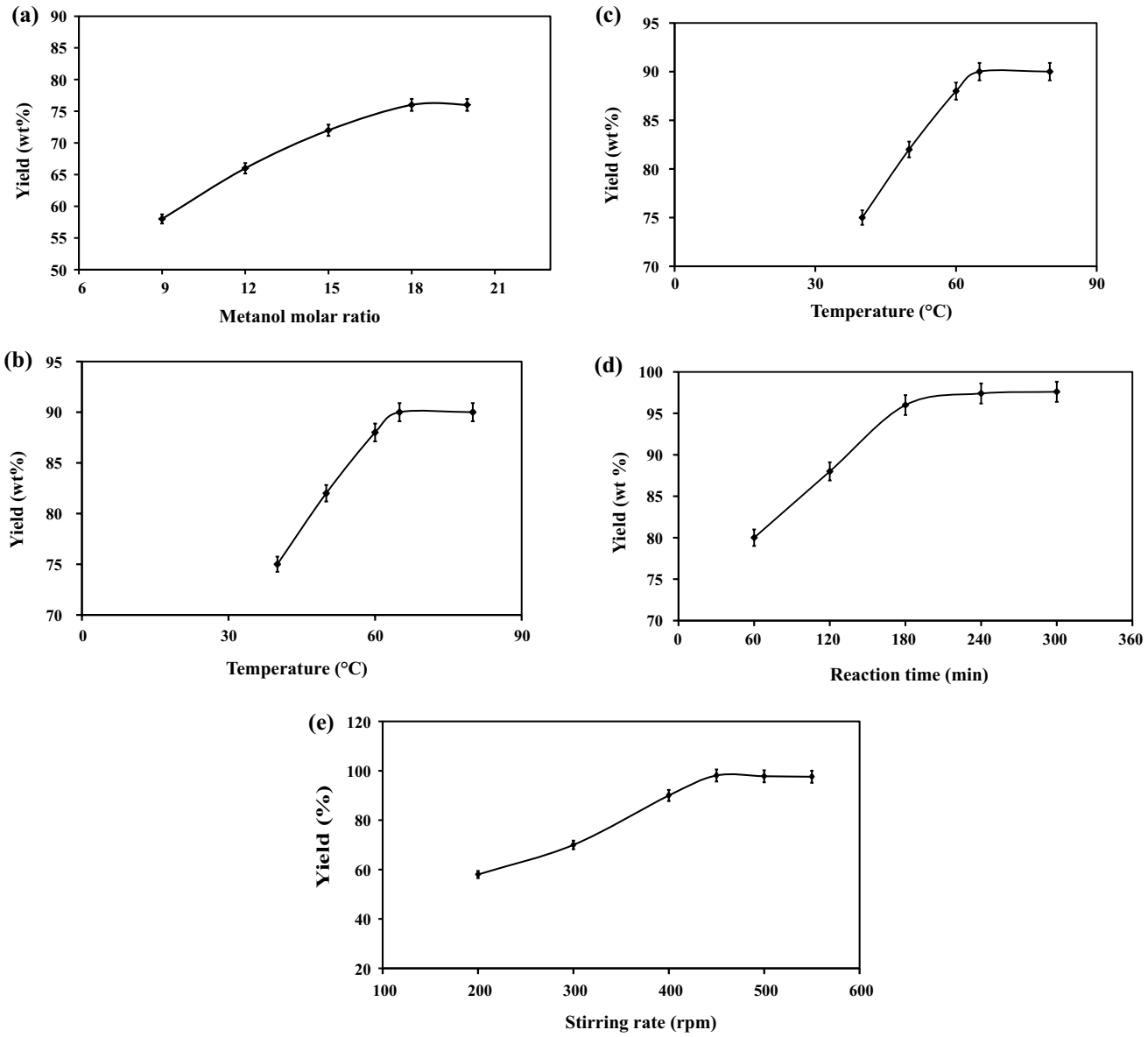

Fig. 4 **a**. Effect of methanol to oil molar ratio (6 wt% catalyst, 60 °C, 240 min, 350 rpm). **b**. Effect of catalyst loading (60 °C, 18:1 methanol to oil molar ratio, 240 min, 350 rpm). **c**. Effect of temperature (8 wt% catalyst, 18:1 methanol to oil molar ratio, 240 min, 350 rpm). **d**. Effect of reaction time (8 wt% catalyst, 18:1 methanol to oil molar ratio, 65° C, 350 rpm). **e**. Effect of stirring rate (8 wt% catalyst, 18:1 methanol to oil molar ratio, 65 °C, 300 min)

production at a considerable varying condition from 1 to 10 wt%. The conversion makes a valuable impact over the synthesized catalyst toward the economic aspects of reaction. The magnetic nano-catalyst provides higher catalytic activity which is due to distribution of magnetic field internally as well as externally upon the catalyst by the magnetons, which is developed through the addition of electric field in turn, induces the rate of conversion at a milder reaction condition. So, actually the rate of conversion starts to increase based on the addition of loading the catalyst, which induces the reaction to happen slowly. The optimum catalyst loading was found to be 8 wt%, significantly producing a yield of 80 wt% (Fig. 4b). When the amount of catalyst was further increased beyond the optimum range, tending to lower the activity of the reaction as well as reduces the mixing of methanol, oil and catalyst thereby initiating to phase separation. This confirms reaction greatly relays on the availability of active basic sites of the synthesized catalyst [32].

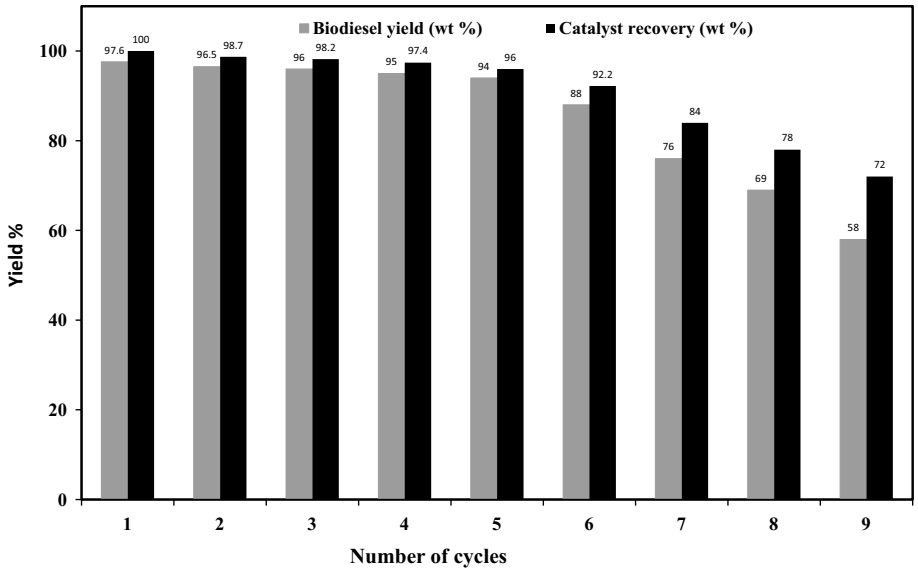

Fig. 5 Reusability of the catalyst (Fe_3O_4/BaO)

3.3.3 Effect of Reaction Temperature

Temperature is an influencing parameter toward the increase in biodiesel yield, which enhances the rate of reaction and conversion. While varying the reaction temperature from 40 to 80 °C during the transesterification reaction, fat tends to liquid form only above 40 °C as well as their seems reduction in viscosity of fat which will induce the miscibility of fat and methanol (Fig. 4c). The improvement in the yield of biodiesel increases while increasing the temperature molecules of the reactant tends to collide at a faster rate promoting toward the activation and attains the highest yield of 90% at 65 °C [33]. The reaction tends to speed up at high temperature provided with the formation of nucleation in turn vaporizing the methanol content and holding the reaction on the interfaces of the reactants, which in turn will reduce the percentage of conversion of biodiesel [22].

3.3.4 Effect of Reaction Time

During the transesterification process, reaction time was investigated by varying it from 30 to 330 min with the optimum catalyst amount of 8 wt%, methanol-to-oil molar ratio of 18:1 and reaction temperature of 65 °C. The increase in yield of biodiesel instantly takes place with respect to increase in the reaction time. This confirms that the mass transfer between the reactant and solubility increases slowly, holding longer reaction time to attain equilibrium (Fig. 4d). A reaction time of 300 min was observed as optimum for producing 97.6% yield of biodiesel. The further increase in reaction time will reverse the reaction because of the reversible nature [34]

3.3.5 Effect of Stirring Intensity

The influence of stirring intensity toward the reaction was investigated in order to observe the optimum range. The yield of biodiesel is found to be varied with respect to stirring rate (Fig. 4e). During the reaction, based on the stirring rate only mass transfer between the reactants increases, which is mainly because of the increase in contact area of the reactant as well as collision between the reactant enhances the conversion of biodiesel [35]. This also causes the reduction in viscosity and helps in forming a phase similar to homogeneous phase. The optimum range was found to be 450 rpm, producing a maximum yield of 98.1% and with further increasing the stirring speed reaction proceeds constantly without any considerable change [36].

3.4 Kinetic Study

The transesterification reaction was carried out by the fat extracted from tannery sludge and methyl alcohol with the utilization of heterogeneous solid catalyst, which occurs at moderate temperature and pressure for performing kinetic studies. It has been observed that the transesterification reaction is a three-phase system constituting fat, methanol and catalyst in turn the reaction is well limited and slows down due to mass transfer (diffusion takes place slowly during the course of the reaction, that is because of the immiscibility of fat with methanol) [37]. The difficult part of the reaction is that fat and methanol take longer time to get dissolved and enables a three-phase reaction mixture with catalyst. For the reaction to takes place, stoichiometry proportion was followed such that one mole of triglyceride requires three moles of methanol for producing three moles of fatty acid methyl ester and one mole of glycerol as shown in Eq. (6). Here, the

reversible reaction takes place, consequently via three steps with the presence of limiting reactant triglyceride (TG) and excess reactant methyl alcohol (MeOH). The excess amount of methyl alcohol was utilized for the reaction in order to precede the reaction toward the right-hand side. The product methyl ester is formed in each step with the intermediates such as diglycerides (DG) and monoglycerides (MG) and finally with the by-product as glycerol (G). The pseudo-first reaction was followed due to the effect of single-step process in which the ester phase in the triglyceride was removed instantly with the addition of methyl alcohol. The assumptions followed in the kinetic studies were (i) intermediate products were kept negligible, (ii) overall reaction occurred in the limiting reactant side, (iii) The rate-limiting step controls the reaction to precede slowly to enhance the rate of conversion, i.e., reaction between triglyceride and methanol [38], (iv) esterification reaction was negligible due to lower concentration of free fatty acid and (v) the influence of the presence glycerides over the surface of the active sites of catalyst.

$$\mathrm{TG} + \mathrm{MeOH} \rightarrow \mathrm{ME} + \mathrm{DG} \tag{6}$$

$$\mathrm{DG} + \mathrm{MeOH} \rightarrow \mathrm{ME} + \mathrm{MG}$$

$$\mathrm{MG} + \mathrm{MeOH} \rightarrow \mathrm{ME} + G$$

$$-r = \frac{-d[\mathrm{TG}]}{dt} = k[\mathrm{TG}][\mathrm{MeOH}]^3 \tag{7}$$

$$k' = k[\mathrm{MeOH}]^3. \tag{8}$$

Equation (7) reduced to the form

$$-r = \frac{-d[\mathrm{TG}]}{dt} = k'[\mathrm{TG}] \tag{9}$$

$$-r = \frac{-d[\mathrm{TG}]}{[\mathrm{TG}]} = k'dt. \tag{10}$$

On integrating Eq. 10.

$$\ln[\mathrm{TG}]_0 - \ln[\mathrm{TG}]_1 = k't \tag{11}$$

$$\frac{\ln[\mathrm{TG}]_0 - \ln[\mathrm{TG}]_1}{t} = k'. \tag{12}$$

Similarly, the mass balance for transesterification is given in Eq. 13.

$$\frac{[\mathrm{TG}]}{[\mathrm{TG}]_0} = 1 - X_{\mathrm{ME}} \tag{13}$$

$$[\mathrm{TG}] = [\mathrm{TG}]_0\left[1 - X_{\mathrm{ME}}\right] \tag{14}$$

Table 3 Kinetics and thermodynamic constants

Temperature (K)	k' (min $^{-1}$)	A (min $^{-1}$)	E_a (kJ mol^{-1})
323	5.9×10^{-3}		
328	8.02×10^{-3}		
333	1.12×10^{-2}	21.3×10^{3}	46.64
338	1.24×10^{-2}		

$$\frac{dX_{\mathrm{ME}}}{dt} = k'\left[1 - X_{\mathrm{ME}}\right] \tag{15}$$

$$\frac{-\ln\left[1 - X_{\mathrm{ME}}\right]}{t} = k'. \tag{16}$$

By following the kinetic model and with the experimental data, upon varying the time (t), the methyl ester concentration (X_{ME}) was determined. Graphically, by plotting between $-ln\left[1 - X_{ME}\right]$ versus reaction temperature, rate constant k' was obtained under the optimum condition as shown in Table 3.

To derive the transesterification reaction, activation energy (E_a) is needed in order to enhance the requirement which is determined using the Arrhenius equation as shown in Eq. (17).

$$k' = \mathrm{A}\, e^{\frac{-E_a}{\mathrm{RT}}}. \tag{17}$$

Integrating Eq. (17),

$$\ln k' = \ln A - \frac{E_a}{R} \times \frac{1}{T} \tag{18}$$

where A is the pre-exponential factor(s^{-1}), E_a is the activation energy (kJ mol^{-1})(s^{-1}), R is the universal gas constant (J mol^{-1} K^{-1}), T is the absolute temperature (K), and k' is the reaction rate constant (s^{-1}). The Arrhenius parameter such as activation energy and pre-exponential values are obtained through plotting a graph between lnk' vs (1/T) and found to be 46.64 kJ mol^{-1} and 21.3×10^3 min^{-1}, respectively. This pre-exponential factor is utilized to determine the collision between the oil, methanol and catalyst upon continuous stirring. From the aforementioned data, it is confirmed that the transesterification process follows pseudo-first-order reaction, which is compared with the result obtained from the proposed kinetic studies of the work carried out in the other literature [22, 39].

Table 4 Fuel properties of biodiesel

Biodiesel property	Unit	Test method	ASTM D6751	Biodiesel
Cetane number	–	ASTM D613	min 47	57
Sulfated ash	mass %	ASTM D874	max 0.02	0.01
Cloud point	° C	ASTM D2500	Report	7
Water content	mass %	ASTM D2709	max 0.05	0.05
Density	kg m^{-3}	ASTM D1298	860–900	878
Flash point	°C	ASTM D93	min 130	152
Kinematic viscosity@40 °C	mm^2 s^{-1}	ASTM D445	1.9–6.0	4.8
Acid number	mg KOH g^{-1}	ASTM D664	max 0.5	0.32

3.5 Characterization of Biodiesel

3.5.1 H^1 NMR Analysis

The characteristic peaks analyzed in H^1 NMR identify and confirm the existence of saturated and unsaturated fatty acids in the fat extracted tannery sludge [7]. Based on the presence of weight percentage of saturated and unsaturated fatty acids, the α- carbonyl hydrogen double band, β-carbonyl hydrogen single band, methyl protons singlets were observed. The conversion of fat from tannery sludge to biodiesel is found to be 98.8 wt%, but the yield of biodiesel obtained was lower than the conversion efficiency which might be because of the separation process [3].

3.5.2 Fuel Properties

The fuel properties of biodiesel obtained from tannery sludge through the treatment process under the optimum reaction conditions were found to be with the applicable range of ASTM D6751 as shown in Table 4. The biodiesel obtained through this study generated high quality as per the standard properties, especially kinematic viscosity, density, acid number, flash point, water content, cetane number, cloud point and sulfated ash. These values were compared with other reported studies [3, 8]

3.6 Catalyst Reusability

The reusability of catalyst was investigated by utilizing it in the transesterification reaction under various cycles. It is one of the influencing parameters which reduces the economic burden in large-scale process. The determination of the reusability catalyst is examined as per its optimum reaction conditions. After completion of the reaction, the catalyst was recovered through washing with alcoholic solvents includes hexane and methanol to remove the deposited particles from the catalyst surface. Then after, the recovered catalyst was dried in an oven for 3 h at 110 °C in order to reuse for the next cycle of reaction. The similar procedure was followed for nine cycles as reported and found there was not much reduction in yield of biodiesel until the seventh cycle and 86 wt% recovery of catalyst was recovered (Fig. 5). Above the seventh cycle, the activity of the catalyst lowers, which was due to the reduction of active sites from the surface of the catalyst, during washing the pores are blocked at a regular interval by the reactant and product. This will be attributed to increase the reaction temperature and pressure and also enhance the viscosity of oil which in turn lowers the quality of biodiesel [40].

4 Conclusion

The nano-catalysts (Fe_3O_4/BaO) were synthesized for the production of biodiesel from the tannery sludge. The magnetite was synthesized through co-precipitation method and through the impregnation of barium oxide with magnetite. The prepared nano-catalyst was investigated for identifying the morphology behavior through different characterizations via SEM, XRD, VSM and FTIR.

The highest yield of 97.6 wt% was obtained indicating excellent performance by the catalyst for producing biodiesel under optimum conditions. The obtained results represented the best operational condition during transesterification reaction with methanol/oil molar ratio of 18:1, catalyst loading of 8 wt%, reaction temperature of 65 °C, reaction time of 300 min and stirring rate of 450 rpm. The catalyst was recovered using an external magnet and resulted that this catalyst can be reused with minor loss in catalytic activity.

The kinetic studies were carried out for determining the rate constant to identify the rate of reaction and show that it follows pseudo-first-order kinetics. The rate constant for different temperatures was calculated to be 5.9×10^{-3} min^{-1}, 8.02×10^{-3} min^{-1}, 1.12×10^{-2} min^{-1} and 1.24×10^{-2} min^{-1} at 323 K, 328 K, 333 K and 338 K as well as the activation and frequency factor were found to be 46.64 kJ mol^{-1} and 21.3×10^{3} min^{-1}. The fuel properties of obtained biodiesel were tested and found to in accordance with the ASTM standards.

Acknowledgements The authors sincerely thank the Centre of Excellence in Solar Energy, Pandit Deendayal Petroleum University, Gandhinagar, 382007, India, and Petroleum Testing Laboratory, RVS College of Engineering and Technology, Coimbatore, India, for providing laboratory facilities.

Funding This research did not receive any specific grant from funding agencies in the public, commercial or not-for-profit sectors.

References

1. Habib, M.S.; Tayyab, M.; Zahoor, S.; Sarkar, B.: Management of animal fat-based biodiesel supply chain under the paradigm of sustainability. Energy Convers. Manag. **225**, 113345 (2020). https://doi.org/10.1016/j.enconman.2020.113345
2. Corsini, F.; Tatsi, E.; Colombo, A.; Dragonetti, C.; Botta, C.; Turri, S.; Griffini, G.: Highly emissive fluorescent silica-based core/shell nanoparticles for efficient and stable luminescent solar concentrators. Nano Energy **80**, 105551 (2021). https://doi.org/10.1016/j.nanoen.2020.105551
3. Vijaya Kumar, B.; Ramesh, K.; Deepalakshmi, S.; Sivakumar, P.: Production of biodiesel from tannery waste using a stable and recyclable nano-catalyst: an optimization and kinetic study. Fuel **260**, 116373 (2020). https://doi.org/10.1016/j.fuel.2019.116373
4. Anand Kumar, S.A.; Sakthinathan, G.; Vignesh, R.; Rajesh Banu, J.; Al-Muhtaseb, A.H.: Optimized transesterification reaction for efficient biodiesel production using Indian oil sardine fish as feedstock. Fuel **253**, 921–929 (2019). https://doi.org/10.1016/j.fuel.2019.04.172
5. Alhassan, F.H.; Rashid, U.; Taufiq-Yap, Y.H.: Ferric-manganese doped sulphated zirconia nanoparticles catalyst for single-step biodiesel production from waste cooking oil : characterization and optimization. Int. J. Green Energy (2014). https://doi.org/10.1080/15435075.2014.966267
6. Andrea Luca, T.; Monica, P.: Leather tanning: life cycle assessment of retanning, fatliquoring and dyeing. J. Clean. Prod. **226**, 720–729 (2019). https://doi.org/10.1016/j.jclepro.2019.03.335
7. Devaraj, K.; Aathika, S.; Mani, Y.; Thanarasu, A.; Periyasamy, K.; Periyaraman, P.; Velayutham, K.; Subramanian, S.: Experimental investigation on cleaner process of enhanced fat-oil extraction from alkaline leather fleshing waste. J. Clean. Prod. **175**, 1–7 (2018). https://doi.org/10.1016/j.jclepro.2017.11.089
8. Kubendran, D.; Aathika, A.R.S.; Amudha, T.; Thiruselvi, D.; Yuvarani, M.; Sivanesan, S.: Utilization of leather fleshing waste as a feedstock for sustainable biodiesel production. Energy Sour. Part A Recover. Util. Environ. Eff. **39**, 1587–1593 (2017). https://doi.org/10.1080/15567036.2017.1349218
9. Sanek, L.; Pecha, J.; Karel, K.; Michaela, B.: Biodiesel production from tannery fleshings: feedstock pretreatment and process modeling. Fuel **148**, 16–24 (2015). https://doi.org/10.1016/j.fuel.2015.01.084
10. Borah, M.J.; Das, A.; Das, V.; Bhuyan, N.; Deka, D.: Transesterification of waste cooking oil for biodiesel production catalyzed by Zn substituted waste egg shell derived CaO nanocatalyst. Fuel **242**, 345–354 (2019). https://doi.org/10.1016/j.fuel.2019.01.060
11. Seffati, K.; Honarvar, B.; Esmaeili, H.; Esfandiari, N.: Enhanced biodiesel production from chicken fat using CaO/CuFe2O4 nanocatalyst and its combination with diesel to improve fuel properties. Fuel **235**, 1238–1244 (2019). https://doi.org/10.1016/j.fuel.2018.08.118
12. Dantas, J.; Leal, E.; Mapossa, A.B.; Cornejo, D.R.; Costa, A.C.F.M.: Magnetic nanocatalysts of Ni0.5Zn0.5Fe2O4 doped with Cu and performance evaluation in transesterification reaction for biodiesel production. Fuel. **191**, 463–471 (2017). https://doi.org/10.1016/j.fuel.2016.11.107
13. Safakish, E.; Nayebzadeh, H.; Saghatoleslami, N.; Kazemifard, S.: Comprehensive assessment of the preparation conditions of a separable magnetic nanocatalyst for biodiesel production from algae. Algal Res. **49**, 101949 (2020). https://doi.org/10.1016/j.algal.2020.101949
14. Chen, M.N.; Mo, L.P.; Cui, Z.S.; Zhang, Z.H.: Magnetic nanocatalysts: synthesis and application in multicomponent reactions. Curr. Opin. Green Sustain. Chem. **15**, 27–37 (2019). https://doi.org/10.1016/j.cogsc.2018.08.009
15. Govan, J.; Gunko, Y.: Recent advances in the application of magnetic nanoparticles as a support for homogeneous catalysts. Nanomaterials. **4**, 222–241 (2014). https://doi.org/10.3390/nano4020222
16. Williams, H.M.: The application of magnetic nanoparticles in the treatment and monitoring of cancer and infectious diseases. Biosci. Horizons Int. J. Stud. Res. **10**, 1–10 (2017). https://doi.org/10.1093/biohorizons/hzx009
17. Ashok, A.; Ratnaji, T.; Kennedy, L.J.; Vijaya, J.J.; Pragash, R.G.: Magnetically recoverable Mg substituted zinc ferrite nanocatalyst for biodiesel production: process optimization, kinetic and thermodynamic analysis. Renew. Energy. **163**, 480–494 (2021). https://doi.org/10.1016/j.renene.2020.08.081
18. Nayebzadeh, H.; Naderi, F.; Rahmanivahid, B.: Assessment the synthesis conditions of separable magnetic spinel nanocatalyst for green fuel production: optimization of transesterification reaction conditions using response surface methodology. Fuel **271**, 117595 (2020). https://doi.org/10.1016/j.fuel.2020.117595
19. Bayat, A.; Baghdadi, M.; Bidhendi, G.N.: Tailored magnetic nano-alumina as an efficient catalyst for transesterification of waste cooking oil: optimization of biodiesel production using response surface methodology. Energy Convers. Manag. **177**, 395–405 (2018). https://doi.org/10.1016/j.enconman.2018.09.086
20. Xie, W.; Huang, M.: Immobilization of *Candida rugosa* lipase onto graphene oxide Fe3O4 nanocomposite: characterization and application for biodiesel production. Energy Convers. Manag. **159**, 42–53 (2018). https://doi.org/10.1016/j.enconman.2018.01.021
21. Lin, T.; Zhao, S.; Niu, S.; Lyu, Z.; Han, K.; Hu, X.: Halloysite nanotube functionalized with La-Ca bimetallic oxides as novel transesterification catalyst for biodiesel production with molecular simulation. Energy Convers. Manag. **220**, 113138 (2020). https://doi.org/10.1016/j.enconman.2020.113138
22. Feyzi, M.; Norouzi, L.: Preparation and kinetic study of magnetic Ca/Fe3O4@SiO2 nanocatalysts for biodiesel production. Renew. Energy. **94**, 579–586 (2016). https://doi.org/10.1016/j.renene.2016.03.086
23. Liu, J.; Liu, M.; Chen, S.; Wang, B.; Chen, J.; Yang, D.P.; Zhang, S.; Du, W.: Conversion of Au(III)-polluted waste eggshell into functional CaO/Au nanocatalyst for biodiesel production. Green Energy Environ. (2021). https://doi.org/10.1016/j.gee.2020.07.019
24. Kumar, B.V.; Ramesh, K.; Sivakumar, P.: Biodiesel production from tannery waste using a nano catalyst (Ferric-Manganese Doped Sulphated Zirconia). Energy Sour. Part A Recover. Util. Environ. Eff. (2019). https://doi.org/10.1080/15567036.2019.1639849
25. Wang, J.; Cao, Z.F.; Ren, H.; Yu, C.; Wang, S.; Li, L.; Zhong, H.: Reactivation of fenton catalytic performance for Fe3O4 catalyst: optimizing the cyclic performance by low voltage electric field. Appl. Surf. Sci. **500**, 144045 (2020). https://doi.org/10.1016/j.apsusc.2019.144045
26. Bazeera, A.Z.; Amrin, M.I.: Synthesis and characterization of barium oxide nanoparticles. IOSR J. Appl. Phys. **01**, 76–80 (2017). https://doi.org/10.9790/4861-17002017680

27. Rahimi, T.; Kahrizi, D.; Feyzi, M.; Ahmadvandi, H.R.; Mostafaei, M.: Catalytic performance of MgO /Fe2O3-SiO2 core-shell magnetic nanocatalyst for biodiesel production of Camelina sativa seed oil: optimization by RSM-CCD method. Ind. Crops Prod. **159**, 113065 (2021). https://doi.org/10.1016/j.indcrop.2020.113065
28. Shi, M.; Zhang, P.; Fan, M.; Jiang, P.; Dong, Y.: Influence of crystal of Fe2O3 in magnetism and activity of nanoparticle CaO@Fe2O3 for biodiesel production. Fuel **197**, 343–347 (2017). https://doi.org/10.1016/j.fuel.2017.02.060
29. Moraes, M.S.A.; Krause, L.C.; da Cunha, M.E.; Faccini, C.S.; de Menezes, E.W.; Veses, R.C.; Rodrigues, M.R.A.; Caramão, E.B.: Tallow biodiesel: properties evaluation and consumption tests in a diesel engine. Energy Fuels **22**, 1949–1954 (2008). https://doi.org/10.1021/ef7006535
30. Roschat, W.; Siritanon, T.; Yoosuk, B.; Promarak, V.: Biodiesel production from palm oil using hydrated lime-derived CaO as a low-cost basic heterogeneous catalyst. Energy Convers. Manag. **108**, 459–467 (2016). https://doi.org/10.1016/j.enconman.2015.11.036
31. Chingakham, C.; David, A.; Sajith, V.: Fe_3O_4 nanoparticle impregnated eggshell as a novel catalyst for enhanced biodiesel production. Chinese J. Chem. Eng. **11**, 02835–2843 (2019). https://doi.org/10.1016/j.cjche.2019.02.022
32. Hu, S.; Guan, Y.; Wang, Y.; Han, H.: Nano-magnetic catalyst KF/CaO-Fe3O4 for biodiesel production. Appl. Energy **88**, 2685–2690 (2011). https://doi.org/10.1016/j.apenergy.2011.02.012
33. Sivakumar, P.; Parthiban, K.S.; Sivakumar, P.; Vinoba, M.; Renganathan, S.: Optimization of extraction process and kinetics of *Sterculia foetida* seed oil and its process augmentation for biodiesel production. Ind. Eng. Chem. Res. **51**, 8992–8998 (2012). https://doi.org/10.1021/ie300882t
34. Lam, M.; Lee, K.T.: Mixed methanol-ethanol technology to produce greener biodiesel from waste cooking oil: a breakthrough for SO42-/SnO 2-SiO2 catalyst. Fuel Process. Technol. **92**, 1639–1645 (2011). https://doi.org/10.1016/j.fuproc.2011.04.012
35. Nautiyal, P.; Subramanian, K.A.; Dastidar, M.G.: Kinetic and thermodynamic studies on biodiesel production from *Spirulina platensis* algae biomass using single stage extraction-transesterification process. Fuel **135**, 228–234 (2014). https://doi.org/10.1016/j.fuel.2014.06.063
36. Kumar, B.V.; Ramesh, K.; Sivakumar, P.; Balasubramanian, R.: Nano-sulfated zirconia catalyzed biodiesel production from tannery waste sheep fat. Environ. Sci. Pollut. Res. **27**, 20598–20605 (2020). https://doi.org/10.1007/s11356-020-07984-1
37. Sahani, S.; Roy, T.; Sharma, Y.C.: Clean and efficient production of biodiesel using barium cerate as a heterogeneous catalyst for the biodiesel production; kinetics and thermodynamic study. J. Clean. Prod. **237**, 117699 (2019). https://doi.org/10.1016/j.jclepro.2019.117699
38. Muthukumaran, C.; Sharmila, G.; Manojkumar, N.; Gnanaprakasam, A.; Sivakumar, V.M.: Optimization and Kinetic Modeling of Biodiesel Production. Elsevier Ltd., Amsterdam (2020)
39. Zhang, L.; Sheng, B.; Xin, Z.; Liu, Q.; Sun, S.: Kinetics of transesterification of palm oil and dimethyl carbonate for biodiesel production at the catalysis of heterogeneous base catalyst. Bioresour. Technol. **101**, 8144–8150 (2010). https://doi.org/10.1016/j.biortech.2010.05.069
40. Rahmani Vahid, B.; Haghighi, M.: Biodiesel production from sunflower oil over MgO/MgAl2O4nanocatalyst: effect of fuel type on catalyst nanostructure and performance. Energy Convers. Manag. **134**, 290–300 (2017). https://doi.org/10.1016/j.enconman.2016.12.048